



CERN - TS Department

EDMS Nr: 629483
Group reference: TS-LEA

TS-Note-2005-052
1 August 2005

Radiation induced effects on the sensors of the Hydrostatic Leveling System for the LHC low beta quadrupoles

E. Dimovasili¹, A. Herty¹, H. Mainaud Durand¹, A. Marin¹, F. Ossart², T. Wijnands¹

¹ CERN 1211 Geneva 23, Switzerland

² FOGALE Nanotech, Parc Kennedy-Bât A3, 285 Rue Gilles Roberval, F-30915, Nimes Cedex

Abstract

The dose rate dependence of the Hydrostatic Leveling System (HLS) for the final focusing quadrupole magnets in the Large Hadron collider is discussed. At high dose rates, ionization of the air inside the sensors causes charge deposition and this perturbs the position measurement. A model is presented that corrects the HLS signal offset as a function of the dose rate. The model compares the HLS with condenser ionization chambers and in this note the results of the comparison are presented.

Keywords: *Low beta quadrupoles, alignment, HLS, radiation, ionization*

CONTENTS

1. Introduction.....	1
2. Hydrostatic Leveling System.....	1
2.1. <i>Operating principles of the HLS</i>	1
2.2 <i>Radiation induced effects</i>	3
3. Experimental set –up.....	4
4. Experimental results.....	5
4.1 <i>Recombination in the sensors</i>	5
4.2 <i>The HLS sensors as condenser ionization chambers</i>	5
4.3. <i>The validity of the calibration polynomials</i>	8
4.4. <i>General recombination in the HLS</i>	9
4.5. <i>The HLS and the LHC radiation environment</i>	10
5. Summary and conclusions.....	10
References.....	11
APPENDIX.....	12

1. Introduction

The Large Hadron Collider (LHC) [1] is a high energy, high intensity proton collider presently under construction at CERN which will become operational in 2007. The ultimate aim of this machine is to inject, accelerate and collide two proton beams of 10^{11} particles head-on each at energy of 7 TeV. At the location where the beams collide, large detectors are used to detect the collision products. A key performance parameter for a detector is the luminosity which is a quantity proportional to the number of collisions per second. In past and present colliders, luminosity is culminated at rate of around $L = 10^{32} \text{cm}^{-2} \text{s}^{-1}$ while in the LHC it will reach $L = 10^{34} \text{cm}^{-2} \text{s}^{-1}$. In order to achieve this goal, it is required to focus the counter rotating beams -before they collide- using 3 quadrupole magnets, the so called inner triplet. The size of the beam is very small and therefore the alignment of the magnets in the inner triplet is very important, concerning both the position of the inner triplet with respect to the detector and the position of the quadrupoles with respect to each other inside the inner triplet.

The Hydrostatic Leveling System (HLS) has been designed to provide relative measurement of the magnet position, in particular the vertical position and transverse tilt. The sensors of the HLS system have to operate reliable in a complex radiation field created by particles that did not collide head-on in the detector but that were deflected by the strong electromagnetic field of the opposing bunch. These so called collision products have a high forward momentum and are usually lost in first few meters after the experimental cavern, i.e. where the inner triplet is located. Under the cryostat of the low beta quadrupoles where the position sensors are located, there is a strong radiation field with dose rates up to 16,000 Gy/year.

During previously conducted aging tests with ^{60}Co , it was found that the HLS sensors show a strong dependence on the dose rate. In this paper, it will be shown that the charge produced by radiation in the air cavity of the HLS, is deposited on the surface of a capacitance and interpreted by the read- out electronics as a movement of a magnet. It will be shown that this can be corrected with the data provided in this note.

2. Hydrostatic Leveling System

2.1. Operating principles of the HLS

The basic principle of the HLS system consists in measuring the water levels in a closed circuit at various locations. The HLS systems that are used for the particle detectors of the LHC are composed of one hundred hydrostatic sensor units¹ (produced by Fogale Nanotech [2]) interconnected with fluid and air pipes and located in referenced points onto the final focusing quadrupoles. The HLS that are used in this study are shown in Figure 1. A cross section of a sensor is shown in Figure 2.

¹ The term *sensor unit* has to be regarded as the ensemble of measuring sensor surface, electronics and connecting cables.



Figure 1. Two different types of HLS sensors (left: 1st generation, right: 4th generation)

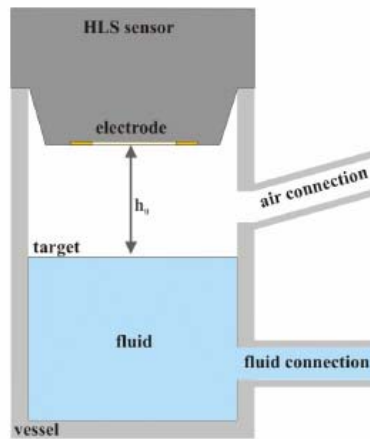


Figure 2. Cross section of a HLS sensor.

The HLS sensors perform hydrostatic leveling measurements with respect to a plane which is the free surface of a water network following the principle of communicating vessels. The continuous monitoring of the relative position is performed by the sensor's surface (electrode) and the water surface (the target). The electrode and the target are separated by air. The electrode is integrated in the top of the vessel. The principle of operation is based on capacitive measurements that determine the distance to the target. When a voltage is applied to one of the plates, the difference between the charge stored on the surfaces of the plates will cause an electric field to exist between them. The amount of existing charge determines the amount of current required to change the voltage on the electrode.

The driver electronics continuously change the voltage on the electrode with an excitation frequency of 4 kHz. The amount of current required to change the voltage on the electrode is detected by the electronics and indicates the amount of capacitance between sensor and target. The change ΔC in capacitance is directly related to the change in the distance between the electrode and the target level [3] as:

$$\Delta C = \frac{\varepsilon_o \cdot \varepsilon_r \cdot S}{\Delta h} \quad (1)$$

where ε_0 the absolute permittivity of free space (8.85×10^{-12}), ε_r the relative permittivity (dielectric constant) of air, S the surface of the electrode and Δh the variation of the distance between the electrode and the target.

The resulting output voltage is given by equation (2) [3]

$$V_{out} = (V_{offset} + \frac{1}{C_e} \cdot V_e \cdot C_{ref}) \cdot G \quad (2)$$

In this formula C_e is the capacitance value during the measurement, C_{ref} is the reference value of the capacitance (i.e the capacitance for a reference distance between electrode and target that was measured during calibration), V_e is the voltage applied between the plates of the capacitor and G is the gain² of the electronics.

The manufacturing company [2] provides calibration polynomials to compute the offset. For each sensor there is a different polynomial. The one for sensor H7D5-361 is given in equation (3) and the others in Table A1 in the Appendix.

$$h [\text{mm}] = 4.999 + 5.010 \cdot 10^{-1} \cdot V_{out} - 2.647 \cdot 10^{-4} \cdot V_{out}^2 + 1.688 \cdot 10^{-5} \cdot V_{out}^3 \quad (3)$$

The three sensors studied here have undergone a calibration procedure by the manufacturing company during which specific voltage changes are recorded for predefined variations of the gap size. The amount of voltage change for a given amount of gap change is called the sensitivity and for the HLS it is 0.2V/ 100 μ m, i.e. for every 100 μ m of change in the gap, the output voltage will change 0.2V.

The ambient temperature is measured continuously as the signal ΔV_{out} needs correction for the vessel and water dilatation.

2.2 Radiation induced effects

The physical process inside the sensor is assumed to be similar to those inside an ionization chamber. The technique is based upon the Bragg Gray principle [4], which states that the absorbed dose in a given material can be estimated from the ionization produced in a small gas-filled cavity within the material. The Bragg-Gray principle is presented in detail in the Appendix. This principle applies here because the secondary electron ranges are long compared to the internal dimensions of the HLS chamber.

Ionizing radiation creates ions and electrons in the air between the electrode and the target. In the presence of the applied potential difference, the ions and electrons move in opposite directions. The charge deposited by the particles on the target plate changes the electric field and varies the excitation voltage. The more the ionization, the more the charge produced and collected on the electrode. The amount of existing charge determines how much the voltage has to vary so as to keep the electric field between the electrode and the target stable. Since some charge is already produced by radiation, the system needs to make less ‘effort’ to charge the electrode.

² Gain is the ratio of signal output from a system to signal input to the system.

At low dose rates, the amount of electron-ion pairs produced in the air between the target and the water level is proportional to the dose. At higher dose rates, more positive and negative ions recombine so that the signal of the HLS eventually saturates.

There are two types of recombination considered in such a chamber: initial (or columnar) recombination and general (or volume) recombination. During initial recombination ions recombine with electrons from the same track while during general recombination ions recombine with electrons from another track.

As the dose rates to the sensors are high, ions are uniformly distributed in the air cavity [5] and therefore general recombination is the dominant effect.

3. Experimental set –up

Three HLS sensors were irradiated with gamma rays from a ^{60}Co source. The source consisted of ten pencil-like sticks with a height of 16 cm and a diameter of 1 cm, with a total activity 13850 Ci. Gamma rays from cobalt-60 are of relatively high energy and have relatively high penetration³ which makes them suitable for these tests. Two different types of HLS were used: the H7D5-361 with a ceramic electrode (1st generation) and the H7D5-372 and H7D5-001, both with a glass electrode (4th generation).

The irradiation was done at different distances from the source so as to vary the dose rate. Measurements were performed at the dose rates 50 Gy/hr, 100 Gy/hr, 500 Gy/hr, 100 Gy/hr and 1500 Gy/hr. The measurements were repeated at the same dose rates but with descending order, i.e from 1500 Gy/hr to 50 Gy/hr, to obtain better statistics of the recorded data. After the end of each irradiation, access was granted so as to change the distance from the source. The data acquisition was performed with two different racks and the data were recorded on two computers, outside the irradiation hall. The HLS electronics were switched on 4 hours before the first irradiation session, for the signal to stabilize. The vacuum pump system was also installed outside the hall in order to be able to perform tests in parallel.

During the experiments the dose rates inside the irradiation hall were monitored by the Radiation Protection Group of the host facility. An independent parallel assessment of the dose received by the sensors (for each dose rate), was also done with the radiophoto luminescent (RPL) glass dosimeters and Alanine dosimeters [6]. The readings of the dosimeters agree within 15% with the reference values. The temperature in the hall remained constant within 10 degrees of Celsius.

³Each disintegration of a ^{60}Co nucleus, which entails the emission of a beta particle, is accompanied by the emission of two gamma photons of energies 1.17 and 1.33 MeV. The gamma photon from ^{60}Co travels a longer distance than a lower-energy gamma photon (e.g. In the case of a ^{137}Cs source).

4. Experimental results

4.1 Recombination in the sensors

Figure 3 shows the variation of the output voltage as a function of the dose rate (see also Figures a-1 and a-2 in the Appendix for the other sensors). This curve indicates the existence of recombination in the sensor; otherwise it should be a straight line. The analysis is described in the next sections only for sensor H7D5-361. The graphs and Tables for sensors H7D5-372 and H7D5-001 are given in the Appendix.

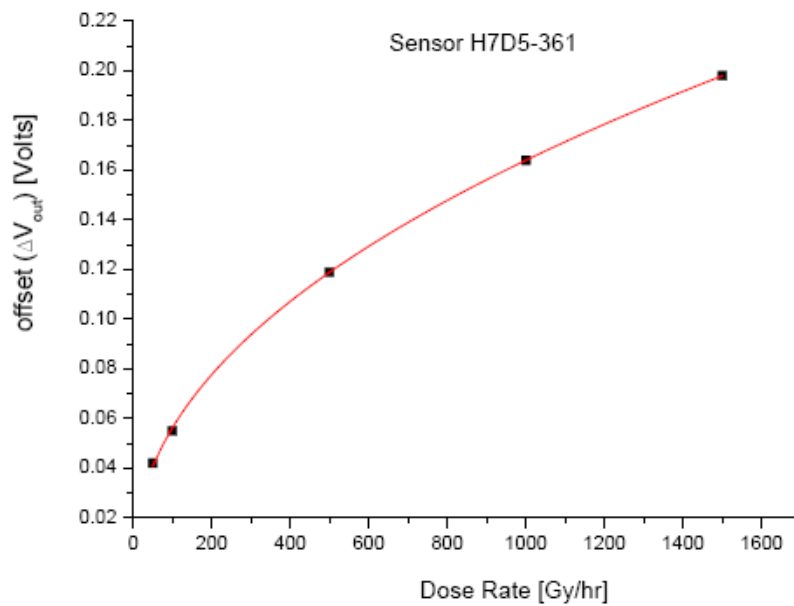


Figure 3. The offset variation of a HLS sensor as a function of the dose rate [Gy/hr] (irradiation with a ^{60}Co source).

4.2 The HLS sensors as condenser ionization chambers

It was initially assumed that the HLS sensors show a similar response with condenser ionization chambers. A condenser chamber is built as a capacitor. A central anode, insulated from the rest of the chamber, is given an initial charge from a charge-reader device. When exposed to photons, the secondary electrons liberated in the walls and enclosed air tend to neutralize the charge on the anode and lower the potential difference between it and the wall. The change in potential difference is directly proportional to the total ionization produced and hence to the exposure. Thus, after exposure to photons, measurement of the change in potential difference from its original value (when the chamber was fully charged) can be used to find the exposure.

The initial assumption that the HLS sensor behaves similarly to condenser chamber and satisfies the Bragg-Gray conditions allows the calculation of the ionization current by the following equation⁴ [7]:

⁴ The reader can find the explanation about the Bragg- Gray principle and the derivation of equation (4) in the Appendix.

$$I_{ion} = \frac{\dot{D} \cdot m \cdot S_g}{W \cdot S_w} \quad (4)$$

where \dot{D} is the dose rate in the air inside the sensor, I_{ion} the induced ionization current, m the mass of air inside the sensor, S_g/S_w the ratio of the mass stopping power of the gas and the wall and W a constant that depends on the gas and it has the value 34.1 J/C for air.

This current was calculated assuming that it is a dc current, that the electric field remains constant and that this current can be added to the one flowing in the circuit. In this case, the ionization current induced in the sensor at all different dose rates was calculated and it is given in the second column of Table 1. The third column is the output voltage reduction ΔV_{out} , that is the difference between the sensor's signal during irradiation, V_{out}^{rad} , and the sensor's signal before the irradiation, V_{out} , i.e.

$$\Delta V_{out} = V_{out}^{rad} - V_{out} \quad (5)$$

In order to verify that the ionization current I_{ion} is related to the output voltage of the HLS sensor, the voltage reduction was also calculated by equation (2). The results are presented in the last column of Table 1 (see Table A2 in the Appendix for the other sensors).

Table 1. The ionization current and the voltage decrease in the H7D5-361 sensor at various dose rates.

\dot{D} [Gy/hr]	I_{ion} [nA] (calculated)	ΔV_{out} [Volts] (measured)	ΔV_{out} [Volts] (calculated)
50	0.50	0.042	0.047
100	1.00	0.055	0.061
500	4.98	0.119	0.132
1000	10.31	0.164	0.183
1500	15.65	0.198	0.221

This table shows that the I_{ion} is not linearly proportional to the offset ΔV_{out} and this verifies the existence of recombination in the HLS sensors.

The ionization current versus the measured output for all different dose rates is shown in Figure 4 along with an exponential growth fit of first order. The errors are less than 0.1% in all cases and it is not possible to show them on the graphs.

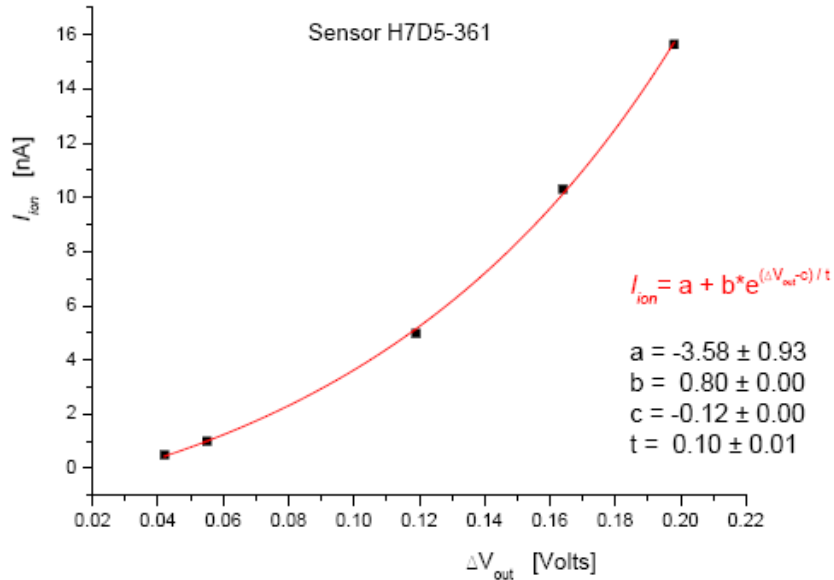


Figure 4. Ionization current versus output potential difference for sensor H7D5-361. The red line is an exponential growth fit of first order.

The corresponding curves for sensors H7D5-372 and H7D5-001 are given in Figures a-3 and a-4 in the Appendix. Figure 5 shows the experimental points for all the sensors and it provides an average polynomial.

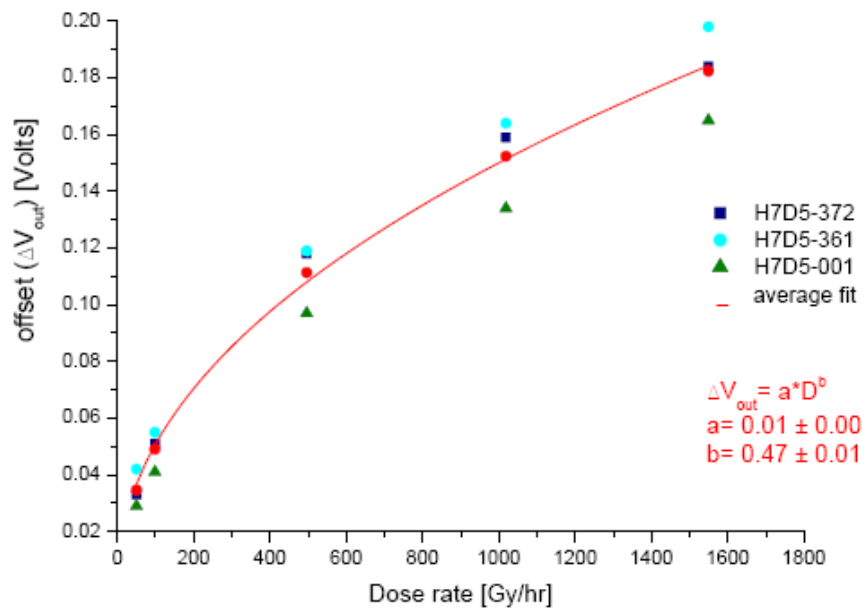


Figure 5. The measured voltage offset for all sensors and the average variation (in red).

4.3. The validity of the calibration polynomials

As discussed in section 2.2, the charge on the electrode is increasing due to ionization in the air inside the sensor and therefore the voltage that is needed to maintain the electric field is reduced. This is interpreted by the electronics as a capacitance change and the output voltage decreases. In other words this effect is due to the electronics design rather than a real ‘internal movement’ of the HLS sensor and it explains the fact that the offset is observed only during the exposure of the HLS to radiation.

To correct the signal, the calibration polynomials can be used. Using equation (2) with the values of the parameters given in Table 2, one can calculate the theoretical variation of capacitance, for different dose rates. Then, by equation (4), the distance between electrode and target can be derived. Since the nominal distance between electrode and target is known (from the value of the capacitance before irradiation), the *hypothetical* offset (in microns) due to radiation can be obtained.

Table 2: Parameters used for the calculation of the capacitance variation.

Parameter	offset [mm] (theoretical)
V_{off}	-4.55
C_{ref}	0.11
V_e	9.00
G	2.23

The offsets that were calculated as described above are denoted as ‘experimental’ while the calculations with the use of polynomials are denoted as ‘theoretical’. The comparison between experimental and theoretical values is given in Table 3 for sensor H7D5-361 (see also Table A3 in the Appendix for the other sensors).

Table 3: Comparison of the two methods (experimental –theoretical) for the offset calculation.

Dose rate [Gy/hr]	Δh [mm] (theoretical)	Δh [mm] (experimental)	Difference (%)
50	21.10	21.06	0.21
100	27.34	27.29	0.21
500	59.18	59.06	0.20
1000	81.79	81.64	0.19
1500	98.96	98.79	0.18

This comparison confirms that the calibration polynomials are valid under irradiation.

4.4. General recombination in the HLS

A proof of the existence of recombination in the chamber is the non linear variation of the collection efficiency of the electrode with radiation [5]. The collection efficiency of a condenser chamber at a voltage V is given by the following equation:

$$f_{av} = \frac{1}{[1 + (1/6\lambda) \cdot \xi_o^2]} \quad (6)$$

where the parameter ξ_o is given by the formula $\xi_o = m \cdot (h^2 \sqrt{q/V_o})$, λ is the ratio of the original voltage over the final voltage (i.e. V/V_o), m a constant depending on the gas in the chamber, h is the distance between electrode and target and q the ionization intensity in units [$\text{esu}/\text{cm}^3/\text{s}$].

It was possible to find in the bibliography [5], curves that predict the collection efficiency at certain dose rates (Figure 6). These curves were calculated in the 80's for condenser ionization chambers and due to lack of high energy experiments at that time, there are no reference data for very high dose rates.

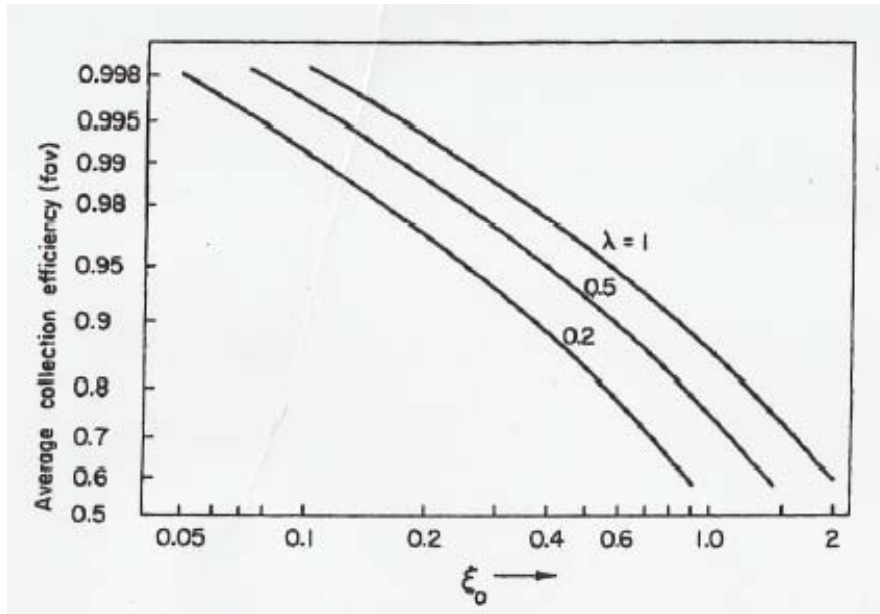


Figure 6. Average collection efficiency of a condenser chamber exposed to continuous radiation. For accuracy in reading, logarithmic scale is used. ξ_o is based on the initial voltage and λ is the ratio of the voltage on the chamber after irradiation to the initial voltage.

The results for the collection efficiency are presented in Table 4 for all sensors. The agreement between the reference data and the calculations is very good and there is no evidence that the reference data provide correct results for low dose rates but not for high ones.

From the collection efficiency one can easily calculate the saturation current I_{sat} . This is given in the third column of Table 4. The I_{sat} is the current that should be measured if all the ions formed in chamber by the radiation were able to reach the electrode. The difference between I_{ion} and I_{sat} indicates the recombination in the

chamber. This is given in the last column of Table 4. The values for the other sensors are given in Table A4 in the Appendix.

Table 4: The collection efficiency of the electrode of HLS (all types). The data are compared with theoretical values derived from graphs in the bibliography [5].

SENSOR 361					
Dose Rate [Gy/hr]	Average calculated collection efficiency f_{av}	Theoretical collection efficiency (bibliography)	$I_{sat} = I_{ion} f_{av}$	ionization current I_{ion} (calculated)	General recombination (%)
50	0.85	0.87	0.56	0.47	16.07
100	0.74	0.77	1.26	0.93	26.19
500	0.37	no exp. data available	12.72	4.66	63.36
1000	0.22		43.73	9.67	77.88
1500	0.16		92.20	14.67	84.09

4.5. The HLS and the LHC radiation environment

The HLS will be installed on the external metrological reference points of the low beta quadrupoles of the LHC, in a very high radiation environment. The ATLAS and CMS experiments involve the highest dose rates and only these cases are considered and discussed. Rough estimates of various radiological parameters associated with the inner triplet of the high luminosity insertions of the LHC can be found in [8, 9]. Monte Carlo calculations have shown that very close to the quadrupoles, any equipment installed will have to resist an irradiation of 16 kGy per year of operation. A year of operation corresponds to around 140 days for production physics. Assuming an optimum run time of 12 hours, it follows that the HLS will have to resist dose rates up to 10 Gy/hr for the first year of the LHC operation. Such dose rates will have no effect on the lifetime of the HLS but as it can be seen by the previous graphs they will provoke an offset of about 10 microns to the HLS reading. The dose rates however will be monitored on line by the RADMON system and a fill-to-fill correction will be possible.

5. Summary and conclusions

The signal from the sensors for the Hydrostatic Leveling System of the LHC will be modified when exposed to ionizing radiation. The radiation induced charge is accumulated on the capacitor plates and provokes a voltage variation in the sensor which is operated at a constant electric field. By assuming a constant ionization current, the HLS can be compared to a condenser type ionization chamber. This model is in good agreement with the experimental data and can be used to predict the HLS offset at arbitrary dose rates.

In addition, the experiments at Saclay have shown that the HLS sensors do not show any signs of aging. The radiation resistance of the HLS electronic readout is approximately 200 Gy Total Ionising Dose and comparable to standard Commercial Off the Shelf Components.

Within the purposes of this technical note it was also possible to verify that the collection efficiency of the electrode varies with the dose and in particular that the approach to saturation depends on the dose rate, a well known effect in condenser ionization chambers.

During the LHC operation, the HLS may show radiation induced offsets of the order of a few microns. The signal of the HLS can be corrected with a model based on the study provided in this note.

References

1. LHC Design Report, Volumes I- III, CERN.
2. <http://www.fogale.fr>
3. F. Ossart, Fogale Nanotech [private communication]
4. Attix F.H., Roesch W.C. and Tochilin E., 'Radiation Dosimetry, II; 9. Academic Press, New York (1966).
5. J. W. Boag, *The Dosimetry of Ionizing Radiation*, edited by K. R. Kase B. E. Bjarngard, and F. H. Attix, Vol. 2 Chap. 3, Academic Press, Orlando, (1987).
6. H. Vincke, SC-RP, CERN (private communication).
7. J. Turner 'Atoms, Radiation and Radiation Protection' Eds J. Wiley & Sons Inc, 2nd Edition, (1995).
8. M. Huhtinen and G.R Stevenson, *Energy deposition, star densities and shielding requirements around the inner triplet of the high luminosity insertions of the LHC*, CERN Divisional Report TIS-RP/IR/95-16 (1995), LHC Note 338.
9. M. Huhtinen and G.R Stevenson, *Estimates of dose to Components in the LHC Tunnel close to the Quadrupoles of the High- luminosity Low- beta regions*, LHC Project Note 22.

APPENDIX

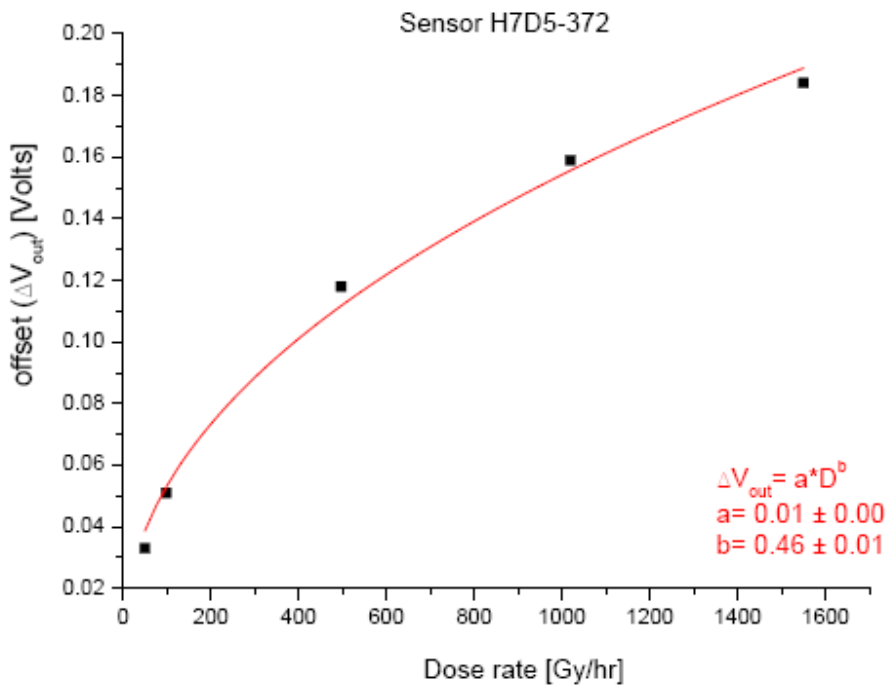


Figure a-1. The offset variation as a function of the dose rate [Gy/hr] (irradiation with a ^{60}Co source).

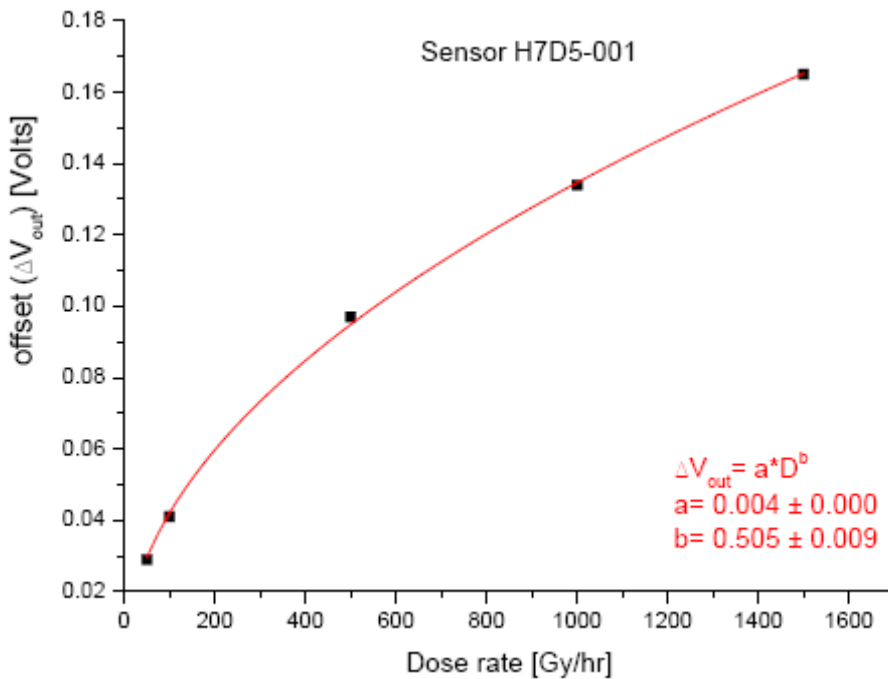


Figure a-2. The offset variation as a function of the dose rate [Gy/hr] (irradiation with a ^{60}Co source).

The Bragg- Gray principle

The Bragg- Gray principle states that if a gas is enclosed by a wall of the same atomic composition and if the wall thickness is not so great to attenuate appreciably the incident radiation, then the energy absorbed per unit mass in the gas is equal to the number of ion pairs produced there times the W value divided by the mass m of the gas. Furthermore, the absorbed dose D_g in the gas is equal to the absorbed dose D_w in the wall. Denoting the number of ions in the gas by N_g , one can write:

$$D_w = D_g = \frac{N_g \cdot W}{m} \quad (i)$$

When the wall and gas are of different atomic composition, the absorbed dose in the wall can still be obtained from the ionization in the gas. In this case, the cavity size and gas pressure must be small, so that secondary charged particles lose only a small fraction of their energy in the gas. The absorbed dose scales as the ratio S_w/S_g of the mass stopping powers of the wall and gas:

$$D_w = \frac{D_g \cdot S_w}{S_g} = \frac{N_g \cdot W \cdot S_w}{m \cdot S_g} \quad (ii)$$

If the dose rate \dot{D} is measured, then equation (ii) becomes

$$\dot{D}_w = \frac{I_{ion} \cdot W \cdot S_w}{m \cdot S_g}$$

where I_{ion} is the ionization current induced by radiation.

Table A1. The calibration polynomials of Fogale Nanotech for the HLS sensors

Sensor	Polynomial ($y \rightarrow$ [mm], $V \rightarrow$ [Volts])
372	$y = 4.99927 + 0.509377 \cdot V - 0.0023040 \cdot V^2 + 0.00013632 \cdot V^3$
001	$y = 4.99913 + 0.508767 \cdot V - 0.0022748 \cdot V^2 + 0.00013938 \cdot V^3$

Table A2.

Type of sensor	Dose rate [Gy/hr]	Ionisation current [nA] (calculated)	dV(Volts) (measured)
H7D5-372 (generation 4)	50	0.50	0.033
	100	1.00	0.051
	500	4.98	0.118
	1000	10.31	0.159
	1500	15.65	0.184
H7D5-001 (generation 2)	50	0.77	0.029
	100	1.53	0.041
	500	7.64	0.097
	1000	15.83	0.134
	1500	24.03	0.165

Table A3: Comparison of the two methods (experimental –theoretical) for the offset calculation.

Sensor	offset [mm] (theoretical)	Offset [mm] (experimental)	Difference (%)
372	16.55	16.53	0.13
	22.12	25.61	15.78
	52.93	58.82	11.12
	73.30	79.03	7.82
	88.87	91.74	3.23
001	14.70	14.71	0.05
	18.02	18.04	0.07
	44.27	44.30	0.07
	61.88	61.92	0.07
	77.18	77.22	0.06

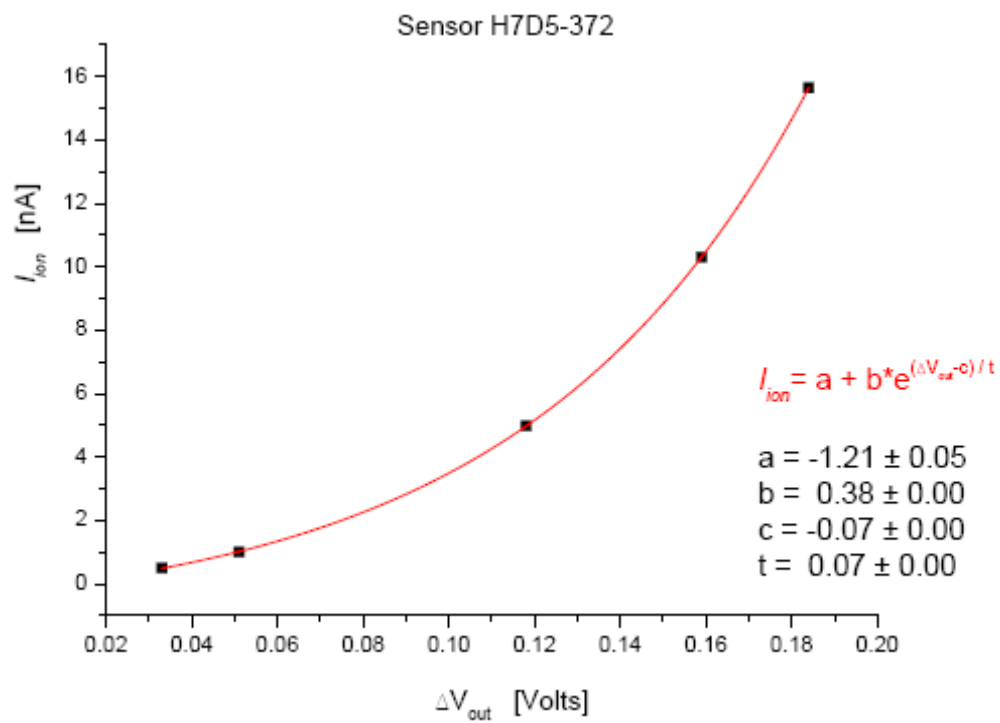


Figure a-3. Ionization current versus output potential difference for sensor H7D5372.

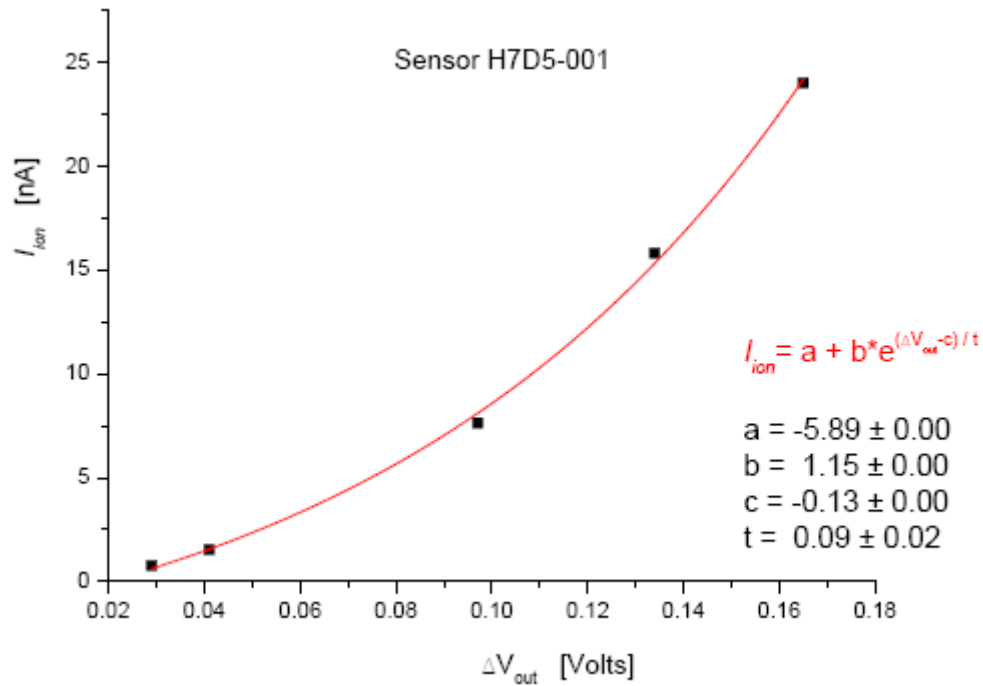


Figure a-4. Ionization current versus output potential difference for sensor H7D5001.

Table A4. The collection efficiency of sensors H7D5-372 and H7D5-001

	f_{av}	Theoretical (bibliography)	$I_s = I / f_{av}$	measured I_{ion}	Recombination (%)
Sensor H7D5372	0.85	0.87	0.59	0.50	15.25
	0.74	0.77	1.35	1.00	26.12
	0.37	no value available	13.57	4.98	63.33
	0.22		46.72	10.31	77.93
	0.16		98.76	15.65	84.15
Sensor H7D5001	0.85	0.87	0.91	0.77	15.07
	0.74	0.77	2.06	1.53	25.88
	0.37	no value available	20.72	7.64	63.12
	0.22		71.22	15.83	77.77
	0.16		149.94	24.03	83.97